

RELATIVISTIC MEAN-FIELD STUDY OF EVEN-EVEN OXYGEN ISOTOPES**J. Leja***Faculty of Mathematics, Physics and Informatics, Comenius University, SK-842 15 Bratislava,
Slovakia***Š. Gmuca***Institute of Physics, Slovak Academy of Sciences, SK-824 28 Bratislava, Slovakia*

Received 9 February 2001, in final form 10 April 2001, accepted 12 April 2001

We have calculated ground-state properties of even–even oxygen isotopes in the framework of the relativistic mean-field theory with three different parameterizations. Calculations have been performed for isotopes from ^{12}O to ^{28}O . The particle stability of very neutron-rich O isotopes is discussed.

PACS: 21.10.Dr, 21.10.Pc, 27.20.+n, 27.30.+t

1 Introduction

Atomic nuclei with extreme isospin values present one of the most active areas of current nuclear physics research. From a theoretical point of view, exotic nuclei offer possibility to study components of nuclear interaction depending on isospin degrees of freedom, which are small in nuclei close to the line of β -stability. In the past years many experiments using radioactive nuclear beams have provided new information on nuclei close to proton and neutron drip-lines and many unusual properties have been revealed (see e.g. ref. [1] for review).

The well known phenomenon is the developing of halo structure. Halo nuclei are characterized by very large sizes with very diffused surfaces implied by weak binding of their last nucleon or nucleons. Halo nucleons lie close to particle continuum, therefore pairing correlations play an important role. In addition, the existence of nuclear halo leads to new collective vibration modes in nuclei, for example a weakly bound halo part may oscillate out of phase with a tightly bound core [2].

The shell structure of some exotic nuclei is characterized by decreasing of spin-orbit splittings leading to uniform distribution of energy levels without big energy gaps between nuclear shells. This phenomenon is referred as shell gap melting and it is a consequence of modification in nuclear density distribution and increasing importance of the pairing effects [2].

Unusual structure of exotic nuclei represents a great challenge for testing nuclear many-body theories. In recent years the relativistic mean-field theory (RMFT) [3–7], the Hartree-Fock-Bogolyubov [8, 9] and the Monte-Carlo shell model [10, 11] have been frequently used for calculations of their properties.

The RMFT has been already proven to be a powerful tool for describing and predicting bulk and single-particle properties of nuclei from proton to neutron drip-line. The RMFT is a relativistic quantum field theory, based on hadronic degrees of freedom, describing nucleons as relativistic particles interacting through effective meson exchange [12–14].

In the present work, the properties of even-even oxygen nuclei from very neutron deficient isotope ^{12}O to very neutron rich isotope ^{28}O have been calculated in the framework of the RMFT by employing several commonly used RMFT parameterizations. The oxygen isotopes far from the β -stability line represent very interesting area today, because many theoretical calculations assume particle stability of very heavy isotopes ^{26}O and ^{28}O contrary to their experimentally confirmed instability [15–17]. Heavy oxygen isotopes are also good candidates for existence of the neutron halo structure [18–20]. In addition, the unclear role of the N=20 closed shell can be studied in the vicinity of the "island of inversion".

2 The relativistic mean-field theory

The model starts from a Lagrangian density including nucleon field (ψ), isoscalar-scalar meson field (σ), isoscalar-vector meson field (ω), isovector-vector meson field (ρ) and electromagnetic field (A), which reads

$$\begin{aligned} \mathcal{L} = & \bar{\psi} \left[i\gamma_\mu \partial^\mu - M + g_\sigma \sigma - g_\omega \gamma_\mu \omega^\mu - g_\rho \gamma_\mu \vec{\rho}^\mu \cdot \vec{\tau} - e\gamma_\mu \frac{(1-\tau_3)}{2} A^\mu \right] \psi + \\ & + \frac{1}{2} \partial_\mu \sigma \partial^\mu \sigma - m_\sigma^2 \sigma^2 - \frac{1}{3} b_\sigma \sigma^3 - \frac{1}{4} c_\sigma \sigma^4 - \frac{1}{4} O^{\mu\nu} O_{\mu\nu} + \frac{1}{2} m_\omega^2 \omega_\mu \omega^\mu + \\ & + \frac{1}{4} c_\omega (\omega_\mu \omega^\mu)^2 - \frac{1}{4} \vec{R}_{\mu\nu} \vec{R}^{\mu\nu} + \frac{1}{2} m_\rho^2 \vec{\rho}_\mu \vec{\rho}^\mu - \frac{1}{4} F_{\mu\nu} F^{\mu\nu}. \end{aligned} \quad (1)$$

The first line describes the free nucleon field, nucleon-mesons interactions and electromagnetic interaction. Next two lines contain free σ -meson, ω -meson, ρ -meson and electromagnetic parts of the Lagrangian density. The Lagrangian density also contains cubic and quartic self-interactions terms for σ -meson field and quartic self-interaction term for ω -meson field. The g_σ , g_ω , g_ρ are nucleon-meson coupling constants and the strengths of the selfinteractions are given by constants b_σ , c_σ and c_ω . The m_σ , m_ω , m_ρ and M denote meson masses and nucleon mass. The field tensors are given by standard expressions

$$F_{\mu\nu} = \partial_\mu A_\nu - \partial_\nu A_\mu, \quad O_{\mu\nu} = \partial_\mu \omega_\nu - \partial_\nu \omega_\mu, \quad \vec{R}_{\mu\nu} = \partial_\mu \vec{\rho}_\nu - \partial_\nu \vec{\rho}_\mu. \quad (2)$$

The field equations follow from the Euler-Lagrange equations in a standard way. Two approximations are necessary for solution of field equations. The first one is the mean-field approximation introduced by replacing the field operators for mesons and electromagnetic fields by their expectation values. The second one is the no-sea approximation realized by exclusion of the filled Dirac sea of negative energy states.

The Dirac spinor for positive energy solution in spherical case can be written in standard form [13]

$$\mathcal{U}_{n\kappa m t}(r) = \begin{pmatrix} i \frac{G_\alpha(r)}{r} \Phi_{\kappa m} \\ - \frac{F_\alpha(r)}{r} \Phi_{-\kappa m} \end{pmatrix} \zeta_t, \quad (3)$$

where G_α and F_α are upper and lower components of nucleon wave function, ζ_t is an isospinor and $\Phi_{\kappa m}$ is a spherical harmonics function. α denotes quantum numbers n , κ and t , where t is the isospin and κ is the Dirac quantum number given by

$$\kappa = \begin{cases} -\left(j - \frac{1}{2}\right) & \text{for } j = l + \frac{1}{2} \\ +\left(j - \frac{1}{2}\right) & \text{for } j = l - \frac{1}{2} \end{cases}. \quad (4)$$

Using this expression we obtain two coupled Dirac equations for upper and lower components of nucleon wave function

$$\left(\frac{d}{dr} + \frac{\kappa}{r}\right) G_\alpha(r) - [M - U(r) - V(r) + E_\alpha] F_\alpha(r) = 0, \quad (5)$$

$$\left(\frac{d}{dr} + \frac{\kappa}{r}\right) F_\alpha(r) - [M - U(r) + V(r) - E_\alpha] G_\alpha(r) = 0, \quad (6)$$

where $U(r)$ is the scalar potential

$$U(r) = g_\sigma \sigma(r), \quad (7)$$

and $V(r)$ denotes the vector potential

$$V(r) = g_\omega \omega_0(r) + g_\rho \tau_3 \rho_0^{(3)}(r) + e \frac{(1 - \tau_3)}{2} A_0(r). \quad (8)$$

The meson and electromagnetic fields obey the radial Laplace equations

$$\frac{d^2}{dr^2} \sigma(r) + \frac{2}{r} \frac{d}{dr} \sigma(r) - m_\sigma^2 \sigma(r) = -g_\sigma \rho_S(r) - b_\sigma \sigma^2(r) - c_\sigma \sigma^3(r), \quad (9)$$

$$\frac{d^2}{dr^2} \omega_0(r) + \frac{2}{r} \frac{d}{dr} \omega_0(r) - m_\omega^2 \omega_0(r) = -g_\omega \rho_V(r) - c_\omega \omega_0^3(r), \quad (10)$$

$$\frac{d^2}{dr^2} \rho_0^{(3)}(r) + \frac{2}{r} \frac{d}{dr} \rho_0^{(3)}(r) - m_\rho^2 \rho_0^{(3)}(r) = -g_\rho \rho_I(r), \quad (11)$$

$$\frac{d^2}{dr^2} A_0(r) + \frac{2}{r} \frac{d}{dr} A_0(r) = -e \rho_C(r). \quad (12)$$

The source terms on right hands of foregoing equations are the scalar density ρ_S , the vector density ρ_V , the isovector density ρ_I and the charge density ρ_C given by

$$\rho_S(r) = \sum_{\alpha}^{occ} \bar{U}_\alpha(r) U_\alpha(r) = \sum_{\alpha}^{occ} \left(\frac{2j_\alpha + 1}{4\pi r^2} \right) [|G_\alpha(r)|^2 - |F_\alpha(r)|^2], \quad (13)$$

$$\rho_V(r) = \sum_{\alpha}^{occ} U_\alpha^+(r) U_\alpha(r) = \sum_{\alpha}^{occ} \left(\frac{2j_\alpha + 1}{4\pi r^2} \right) [|G_\alpha(r)|^2 + |F_\alpha(r)|^2], \quad (14)$$

$$\rho_I(r) = \sum_{\alpha}^{occ} U_{\alpha}^+(r) \tau_3 U_{\alpha}(r) = \sum_{\alpha}^{occ} \left(\frac{2j_{\alpha} + 1}{4\pi r^2} \right) \tau_3 \left[|G_{\alpha}(r)|^2 + |F_{\alpha}(r)|^2 \right], \quad (15)$$

$$\begin{aligned} \rho_C(r) &= \sum_{\alpha}^{occ} U_{\alpha}^+(r) \frac{(1 - \tau_3)}{2} U_{\alpha}(r) \\ &= \sum_{\alpha}^{occ} \left(\frac{2j_{\alpha} + 1}{4\pi r^2} \right) \frac{(1 - \tau_3)}{2} \left[|G_{\alpha}(r)|^2 + |F_{\alpha}(r)|^2 \right]. \end{aligned} \quad (16)$$

The sums are taken over all occupied states and α is a set of all quantum numbers.

The expression for the total energy can be derived from Lagrangian density and it has a structure,

$$\begin{aligned} E = \sum_{\alpha}^{occ} E_{\alpha} (2j_{\alpha} + 1) - \frac{1}{2} \int \left(g_{\sigma} \sigma_0 \rho_S + g_{\omega} \omega_0 \rho_V + g_{\rho} \rho_0^{(3)} \rho_I + e A_0 \rho_C \right) d^3x + \\ - \int \left(\frac{1}{3} b_{\sigma} \sigma_0^3 + \frac{1}{4} c_{\sigma} \sigma_0^4 - \frac{1}{4} c_{\omega} \omega_0^4 \right) d^3x \end{aligned} \quad (17)$$

The set of Dirac equations (5 – 6) for nucleons and Laplace equations (9 – 12) for mesons and electromagnetic field with expressions for source terms (13 – 16) are solved self-consistently. In addition, the BCS pairing is applied using a constant pairing strength approximation for open shell nuclei and the pairing energy and the correction for the spurious centre of mass motion are added to the total energy.

Table I. Parameters of the RMFT effective forces used in the present investigation.

parameter	NL3	NL-Z2	NL-BA
	Ref. [21]	Ref. [22]	Ref. [23]
M (MeV)	939.0	938.9	939.0
m_{σ} (MeV)	508.194	483.15	506.28
m_{ω} (MeV)	782.501	780.0	782.6
m_{ρ} (MeV)	763.0	763.0	769.0
g_{σ}	10.2169	10.1369	10.129758
g_{ω}	12.8675	12.9084	12.722198
g_{ρ}	4.4744	4.55627	4.508614
b_{σ} (fm $^{-1}$)	-10.4307	-13.7561	-11.480161
c_{σ}	-28.8851	-41.4013	-32.277332

3 Results and discussion

We have calculated the ground-state properties of the even-mass oxygen isotopes with three different RMFT parameterizations, namely NL3 [21], NL-Z2 [22] and NL-BA [23]. The values

Table II. The nuclear matter properties calculated by the RMFT parameter sets used in the present work.

	NL3 [21]	NL-Z2 [22]	NL-BA [23]
saturation density ρ_0 (fm $^{-3}$)	0.148	0.151	0.1503
bulk binding energy/nucleon E_∞/A (MeV)	-16.24	-16.07	-16.1949
incompressibility K (MeV)	272	172	248
bulk symmetry energy/nucleon a_{sym} (MeV)	37.4	39.0	37.7
effective mass ratio M^*/M	0.60	0.58	0.60

of the parameters used are listed in Table I, and the predicted nuclear matter properties are given in Table II. The pairing strength for neutron was set to be $G_n = 7.80/A$ (MeV), which is the average strength for this isotopic chain obtained by fitting the odd-even mass differences.

The recent NL3 parameterization was aimed to improve further the properties of the successful NL-SH [24] parameter set. For this reason a new multiparameter fit was performed. The set of nuclei in the fit was slightly enlarged. The resulting parameters provide improved results over the NL-SH set, reducing the root-mean-square deviation of the binding energies. The nuclear matter incompressibility (K) decreased from $K=355$ MeV (NL-SH) to much lower value $K=272$ MeV (NL3). The NL3 was extensively applied throughout of the chart of nuclides including neutron-rich nuclei and superheavy elements [5].

The parameter set NL-Z2 belongs to the family of completely new RMFT parameterizations provided by the Frankfurt group. It stems from a fit using enlarged set of data including information on exotic nuclei. A microscopic treatment of the correction for the spurious center-of-mass motion was applied. Additionally, the nuclear surface thicknesses were included into the data, providing new information about the nuclear shapes. A distinct feature of this set is a quite low value of the nuclear matter incompressibility coefficient $K=172$ MeV.

The NL-BA parameterization [23] is the freshly new set dealing with a fit to a large body of observables related to ground-state properties of selected doubly-magic nuclei covering a wide variation of isospin. The predicted properties of nuclear matter indicate improvement for the incompressibility coefficient ($K=248$ MeV), while the symmetry energy a_{sym} remains practically the same as in the previous parameterizations.

Our present RMFT application consists of the spherical¹ relativistic mean-field calculation with the parameters sets which have not been used in this region before. All calculations have been performed for even-even oxygen nuclei ranging from ^{12}O to ^{28}O .

Table III summarizes the calculated ground-state binding energies for all three parameterizations. For the NL-Z2 set we did not obtain the convergence for the ^{14}O nucleus. This value is, therefore, absent in Table III. All other results can be compared with the evaluated values [26]. The corresponding binding energy differences between theoretical and experimental data, $\text{BE}_{th} - \text{BE}_{exp}$, are drawn in Fig. 1.

All three parameterizations exhibit similar pattern with seemingly the best agreement given by the NL-BA set. This parameterization describes well the ground-state binding energies for isotopes $^{12-22}\text{O}$; the deviations between calculated and experimental data are well bellow 1 MeV. It is particularly interesting that the binding energy of the extremely proton-rich ^{12}O is

¹Calculations with an axially deformed code gave no indication of deformation for the oxygen isotopes ground states.

Table III. Calculated and experimental [26] binding energies for even-even oxygen isotopes from ^{12}O to ^{28}O . Data flagged with # refer to extrapolation of experimental values.

Isotope	BE [MeV] NL3	BE [MeV] NL-Z2	BE [MeV] NL-BA	BE [MeV] exp.
^{12}O	61.125	60.818	59.919	58.549
^{14}O	100.242	—	98.376	98.733
^{16}O	128.791	127.791	127.390	127.619
^{18}O	141.101	140.643	139.909	139.807
^{20}O	152.300	152.161	151.247	151.371
^{22}O	163.173	163.082	162.159	162.032
^{24}O	171.567	173.056	170.964	168.484
^{26}O	175.488	177.681	175.168	#168.324
^{28}O	179.619	182.711	179.606	#163.464

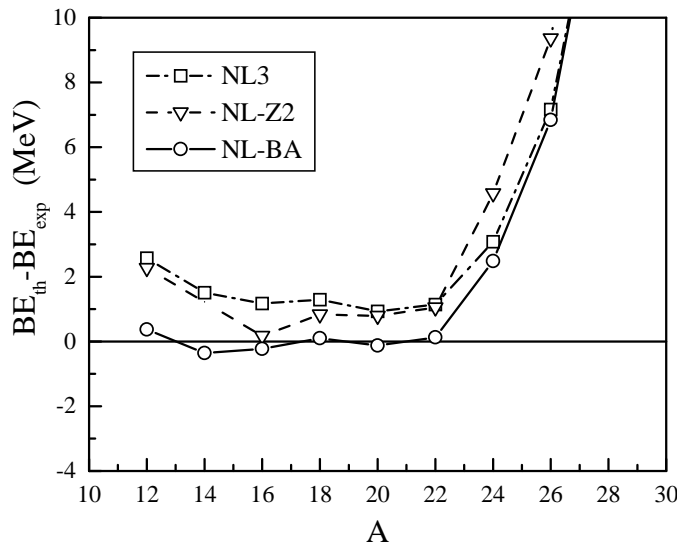


Fig. 1. Binding energy differences for O isotopes.

reproduced so well. The ^{12}O nucleus is unstable against proton emission and lies, therefore, beyond the proton drip line.

The situation on a very neutron-rich side of the O isotopic chain is less satisfactory.

The particle stability of the neutron-rich O nuclei was studied extensively by both, theoretically and experimentally. While recent evaluation of experimental masses by Audi *et al.* [25, 26] indicates that the heaviest O isotopes stable against particle emission is ^{24}O , many of global systematics and mean-field approaches predict that even ^{26}O and ^{28}O are stable. In particular, the finite-range droplet model (FRDM) of Möller *et al.* [27] and Thomas–Fermi systematics of Myers and Swiatecki [28] predict the ^{26}O to be stable against neutron emission. The recent non-

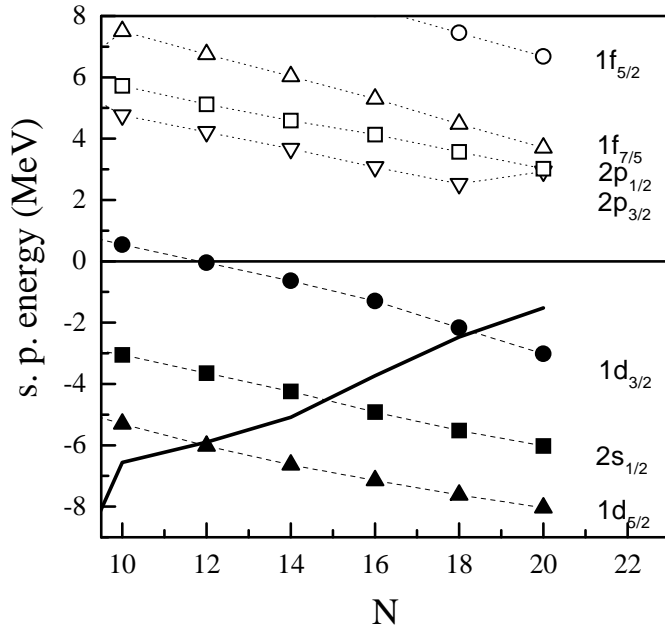


Fig. 2. The neutron single-particle levels of O isotopes calculated with the NL-BA parameters. The thick solid line denotes the neutron Fermi level.

relativistic Hartree–Fock calculations with various Skyrme forces [20, 29, 30] also predict that the $^{26,28}\text{O}$ nuclei are stable (with an exception for a Z_σ^* [31] interaction; in this case the ^{24}O is the heaviest particle-stable isotope). The previous relativistic mean-field calculations [18, 32] again put the ^{28}O on the neutron drip line. In addition, the recent Monte-Carlo shell model approach [33] have demonstrated that the interplay between T=1 and T=0 monopole interactions is essential to reproduce the neutron drip line of O isotopes.

From the experimental point of view, the situation on the neutron-rich side of O isotopic chain is now quite clear. The heaviest O isotope ever observed is ^{24}O . Any attempts to produce the ^{26}O or ^{28}O nuclei were unsuccessful [15, 16]. The clear evidence for the particle instability of $^{26,28}\text{O}$ has been obtained [17, 34].

In contrast, our calculations predict that both, the $^{26,28}\text{O}$ are particle stable for all three parameterizations used, in accord with most of the other mean-field approaches. By inspecting the Fig. 1 we see that deviations between calculated and experimental data start to diverge steeply for the ^{24}O and heavier O isotopes ². We note, that such a behaviour of mean-field model calculations indicates reaching the limit of applicability (validity) of the model (parameterization) used. Similar tendency can be seen also in the global systematics when extrapolating outside of their range of applicability [35].

For deeper understanding of the reasons for the failure of the RMFT model to describe the

²In fact we do not know the experimental masses of $^{26,28}\text{O}$. For these isotopes we are comparing the calculations with extrapolated data of Nubase [26].

neutron drip line of the O element, we study the dependence of the neutron single-particle energies around the Fermi level on the neutron number N . In Fig. 2 we draw this dependence for the bound $1d_{5/2}$, $2s_{1/2}$ and $1d_{3/2}$ states, as well as for the triplet of the unoccupied $1f_{7/2}$, $2p_{3/2}$, $2p_{1/2}$ levels lying in the continuum. Other deep hole states or the continuum levels, are too far away from the Fermi level and, therefore, are unimportant for the present discussion.

Two points are essential for the position of the neutron drip line:

- (1) the $1d_{3/2}$ orbital is too deeply bound,
- (2) the $1f_{7/2}$, $2p_{3/2}$, $2p_{1/2}$ states are too high in the continuum.

Thus, as the $1d_{3/2}$ state starts to fill at $N = 18$, the pairing interaction does not have enough strength to populate the continuum triplet. This leads to the particle stability of $N = 18$ and $N = 20$ for the NL-BA parameters (the same is true also for NL3 and NL-Z2 interaction and, probably, also for other RMFT parameterizations presently used).

To correctly reproduce the experimentally determined neutron drip line of O isotopes we thus need the RMFT interaction that moves the $1d_{3/2}$ level closer to the continuum³ and the triplet of unoccupied continuum states closer to the Fermi level. Whether this can be achieved by (1) a fine tuning of existing parameterizations, or (2) seeking for a completely new RMFT interaction, or even (3) by a modification of the presently used RMF Lagrangian is left for further investigation. We note, that any attempt to move the $1d_{3/2}$ level (and, probably, also the $2s_{1/2}$ one) close to the continuum results in a disappearance of the $N = 20$ magic number. Recent speculations about the existence of new shell closures at $N = 16$ [36], or $N = 14$ [37] provide the support in favor of the reasoning given above. In any case, the very neutron-rich region of O and neighboring nuclei seems to be a promising laboratory for testing the isovector properties of the RMFT approach.

4 Summary

In this work, we have studied the ground state properties of even-even O isotopes by a relativistic mean-field approach with pairing correlation using three new RMFT parameterizations. For most nuclei, the calculation successfully reproduced their binding energies, with the best agreement obtained by the NL-BA parameter set. As the $N = 20$ is approached the agreement breaks down, and the deviations between calculated and experimental data start to diverge steeply for all three parameter sets used. This failure may be due to reaching the limit of applicability (validity) of current RMFT parameterizations for the nuclei with extreme proton to neutron N/Z ratio. The heavy isotopes ^{26}O and ^{28}O are predicted to be particle stable in contrast with the experimental evidences of their instability. This indicates that the correlations beyond the simple mean-field model may play an important role in this region. The relativistic Hartree-Bogolyubov calculations will be worth in this case, and also other long-range correlations should be studied to resolve the discrepancy. The new parameter set with better isovector properties is needed to reproduce the neutron drip line in the O isotopic chain.

³The only successful Skyrme–Hartree–Fock calculation [20] with the Z_σ^* force [31] that correctly predicts ^{24}O to be the neutron drip nucleus, even puts the $1d_{3/2}$ level into the continuum. This leads to the particle instability when this state starts to fill at $N = 18$ and $N = 20$.

5 Acknowledgments

This work was supported in part by the Slovak Grant Agency for Science VEGA under grant No. 2/1132/21. Calculations were partly performed at the Computation Centre of Slovak Academy of Sciences.

References

- [1] I. Tanihata: *J. of Phys. G* **22** (1996) 157
- [2] W. Nazarewicz: *Proc. of Int. Conf. on Fission and Properties of Neutron-Rich Nuclei, November 10-15, 1997, Sanibel Island, USA*, J.H. Hamilton and A.V. Ramayya (eds), World Sci., Singapore 1998, p. 32
- [3] Z. Ren, Z.Y. Zhu, Y.H. Cai, G. Xu: *Nucl. Phys. A* **605** (1996) 75
- [4] Z. Ren, A. Faessler, A. Bobyk: *Phys. Rev. C* **57** (1998) 2752
- [5] G.A. Lalazissis, S. Raman: *Phys. Rev. C* **58** (1998) 1467
- [6] B. Q. Chen, Z. Y. Ma, F. Grüninger, S. Krewald: *J. of Phys. G* **24** (1998) 97
- [7] M. M. Sharma, S. Mythili, A. R. Farhan: *Phys. Rev. C* **59** (1999) 1379
- [8] I. Hamamoto, H. Sagawa, X. Z. Zhang: *Phys. Rev. C* **53** (1996) 765
- [9] N. Nazarewicz et al.: *Phys. Rev. C* **53** (1996) 740
- [10] T. Otsuka, T. Mizusaki, Y. Utsuno and M. Honma: *Proc. of Int. Conf. on Fission and Properties of Neutron-Rich Nuclei, November 10-15. 1997, Sanibel Island, USA*, J. H. Hamilton and A. V. Ramayya (eds), World Sci., Singapore 1998, p. 391
- [11] D. J. Dean: *Phys. Rev. C* **59** (1999) 2474
- [12] W. Greiner, J. A. Maruhn: *Nuclear Models*, Springer-Verlag, Berlin-Heidelberg 1996
- [13] B. D. Serot, J. D. Walecka: *Adv. Nucl. Phys.* **16** (1986) 1
- [14] B. D. Serot, J. D. Walecka: *Int. J. of Mod. Phys. E* **6** (1997) 515
- [15] M. Fauerbach et al.: *Phys. Rev. C* **53** (1996) 647
- [16] O. Tarasov et al.: *Phys. Lett. B* **409** (1997) 64
- [17] H. Sakurai et al.: *Phys. Lett. B* **448** (1999) 180
- [18] Zhongzhou Ren, W. Mittig, Baoqiu Chen, Zhongyu Ma: *Phys. Rev. C* **52** (1995) R20
- [19] R. Bhattacharya, K. Krishan: *Phys. Rev. C* **56** (1997) 212
- [20] T. Siiskonen, P.O. Lipas, J. Rikovska: *Phys. Rev. C* **60** (1999) 034312
- [21] G. A. Lalazissis, J. König, P. Ring: *Phys. Rev. C* **55** (1997) 540
- [22] M. Bender et al.: *Phys. Rev. C* **60** (1999) 034304
- [23] Š. Gmuca: in *Proc. 2nd Int. Conf. Fission and Properties of Neutron-Rich Nuclei, St. Andrews, Scotland, June 28 – July 3, 1999* (Eds. J.H. Hamilton, W.R. Phillips and H.K. Carter). World Sci., Singapore 2000, p. 75;
- [24] M.M. Sharma, M.A. Nagarajan, P. Ring: *Phys. Lett. B* **312** (1993) 377
- [25] G. Audi, A. H. Wapstra: *Nucl. Phys. A* **595** (1995) 409
- [26] G. Audi, O. Bersillon, J. Blachot and A.H. Wapstra: *Nucl. Phys. A* **624** (1997) 1
- [27] P. Möller, J.R. Nix, W.D. Myers, W.J. Swiatecki: *At. Data Nucl. Data Tables* **59** (1995) 185
- [28] W.D. Myers, W.J. Swiatecki: *Report LBL-36803, Berkeley* (1994)
- [29] Naoki Tajima, Satoshi Takahara, Naoki Onishi: *Nucl. Phys. A* **603** (1996) 23

- [30] Xinhua Bai, Jimin Hu: *Phys. Rev. C* **56** (1997) 1410
- [31] J. Friedrich, P.-G. Reinhard: *Phys. Rev. C* **33** (1986) 335
- [32] S.K. Patra: *Nucl. Phys. A* **559** (1993) 173
- [33] Yutaka Utsuno, Takaharu Otsuka, Takahiro Mizusaki, Michio Honma: *Phys. Rev. C* **60** (1999) 054315
- [34] A. Ozawa *et al.*: *Nucl. Phys. A* **673** (2000) 411
- [35] M.D. Lunney *et al.*: in *Proc. Int. Workshop on Research with Fission Fragments, Benediktbeuern, Oct. 1996* (Eds. T. von Egidy *et al.*). World Sci., Singapore 1997, p. 225;
- [36] A. Ozawa *et al.*: *Phys. Rev. Lett.* **84** (2000) 5493
- [37] P.G. Thirolf *et al.*: *Phys. Lett. B* **485** (2000) 16